Journal of Asian Concrete Federation
Vol. 7, No. 1, pp. 24-37, June. 2021
ISSN 2465-7964 / eISSN 2465-7972
DOI http://dx.doi.org/10.18702/acf.2021.06.7.1.24

Assessment of a fire damaged reinforced concrete building

Arup Ghatak, P N Ojha, Brijesh Singh*, Abhishek Singh, TVG Reddy, B N Mohapatra

(Received Feburary 19, 2021; Accepted May 24, 2021; Published online June 30, 2021)

Abstract: A proper condition assessment of reinforced concrete structure after a fire event involves field and laboratory work to determine the extent of fire in order to design an appropriate and cost effective repair scheme. The present paper presents a case study where an attempt has been made to carry out a condition assessment of a fire damaged building in a systematic manner. The approach adopted broadly consisted of questioning of on-site personnel, a detailed visual survey, on-site non-destructive / partially-destructive tests, collection of in-situ samples from site along with some laboratory based investigations on samples collected from site. Differential Thermal Analysis (DTA), X-Ray Diffraction (XRD) Analysis and Scanning Electron Microscopy (SEM) Imaging were conducted for microstructural characterization and analysis of concrete to correlate, corroborate and validate the results obtained through on-site assessment. Since the building was an old structure, carbonation depth in structural members was also evaluated. Finally, based on the visual inspections indicating the condition of surface and structural elements such as spalling, exposure and condition of reinforcement, cracks, honeycombing etc. along with Non-Destructive Test / Laboratory test results, the repair methodology of structural members are presented.

Keywords: Fire, Reinforced Concrete, Condition Assessment, Repair

1. Introduction

Damage to buildings due to fire can potentially be a significant detriment to the structural safety and serviceability of the building. Some catastrophic failures have occurred in recent times on account of damage caused due to breakout and the spread of fire. With the future trend in building construction being more inclined towards high rise buildings, the possibility of damage due to fires is likely to increase. In a large number of cases, concrete buildings are capable of being repaired rather than demolished even after exposure to a severe fire which can lead to significant cost savings as compared to going in for demolition and reconstruction. This is because concrete generally performs well under exposure to fire and is a poor conductor of heat. Due to heterogeneous nature of concrete, each material present in it interacts differently at elevated temperature; hence the properties of concrete as a whole may change radically when exposed to fire. There are changes in chemical and physical properties that may result in undesirable structural failures. The effect of fire on concrete is significantly influenced by coarse aggregate types. Siliceous aggregate concrete retains approximately half its capacity at 650ºC, whereas carbonate and light weight aggregate concrete exhibit near full capacity at 650ºC [1,2]. The thermal protection of reinforcing steel is critical; testing indicates that bars heated beyond 500ºC lose significant amounts of yield strength and ultimate strength [1,2]. Reinforced concrete (RC) structures damaged due to fire require damage assessment, evaluation and repair. There are several techniques and tools available for the structural health assessment of structures. This process includes a comprehensive evaluation consisting of visual inspection, Non-Destructive Testing (NDT) and laboratory testing to evaluate the extent of damage and the level of temperature to which the structural elements have been exposed. The objective of the evaluation shall be to identify the type and extent of fire damage along with evaluating any changes in the physical or material properties in the reinforcing steel and concrete. Ultrasonic pulse velocity (UPV) test, a NDT method, is widely used for the evaluation of the quality of a concrete structure. The UPV measurements made on a structure will provide a qualitative estimation of the damaged members with the undamaged ones [3, 4]. Cioni et al. [5] used thermo-mechanical and microstructural analysis of RC elements along with UPV Method for assessment of fire damaged RC structural elements. From the identified

***Corresponding author* **Brijesh Singh** *is a Group Manager at National Council for Cement and Building Materials, India*
Arup Ghatak *is a Manager at National Council for Cement and Building Materials, India*
P N Ojha *is a Joint director & Head-CDR at National Council for Cement and Building Materials, India*
Abhishek Singh *is a Project Engineer at National Council for Cement and Building Materials, India*
T V G Reddy is *Ex. General Manager at National Council for Cement and Building Materials, India*
B N Mohapatra is Director General at *National Council for Cement and Building Materials, India*

damaged zones, cores can be drilled for further investigation in the laboratory. Wei–Ming Lin studied the microstructure of fire damaged concrete samples using Scanning Electron Microscope and a stereo microscope to estimate the temperature [6]. Short investigated concrete core samples to estimate the temperature and also the depth of damage using color image analysis [7]. Optical microscopy has been used to determine the depth of damage based on the crack density measurements by Georgali et al. [8] The investigation using methods mentioned above are conducted in the laboratory on samples collected from the fire damaged structure.

The evaluation determines the nature and extent of the fire damage and whether repairs are required. This process involves (1) determining when to observe the fire damaged structure (both before and after cleaning), (2) how to evaluate the post fire conditions (visually, non-destructively, or destructively), and (3) assessing the structure to determine what, if any, repairs are required [9, 10]. The three stages of evaluation are visual assessment, NDT and partially-destructive testing. These evaluations, combined with engineering analysis, allow effective and economical repair details to be developed and executed as needed [11, 12]. RC structure which is damaged due to fire can be rehabilitated and strengthened by using various retrofitting methods. Different structural and non-structural members of fire damaged structure are subjected to different repair mechanisms depending upon extent of damages. For example, strengthening of fire damaged RC beams and columns with fiber-reinforced polymer (FRP) sheets [13, 14] and the use of near-surface mounted carbon FRP rods [15] for the repair of damaged slabs are some of the most popular retrofitting methods nowadays. They are sufficiently effective to restore the structural functions of the damaged structural components. In this study, post fire assessment of a RC multi-storey building was conducted through visual survey, different field investigations and several laboratory investigations on samples collected from the fire damaged structure.

2. Experimental program adopted for post fire assessment

Condition assessment of an existing building irrespective of the cause of damage broadly involves collection of data and records, a detailed visual survey, on-site non-destructive/partially-destructive tests, some laboratory based investigations on samples collected from site, etc. In the present case, the post fire assessment of the fire damaged portion of an RC building was carried out in a detailed manner similar to past studies done on fire damaged concrete structures. The condition assessment broadly involved the following stages:

2.1 Collection of data and records

All data available regarding the building was collected. Visual inspection and questioning of on-site staff was done to gather data as neither structural drawings, structural/design details nor were any records available about the materials used for construction.

2.2 Visual survey

A detailed visual survey of the building was carried out. This involved recording details of visual inspection and distress mapping is done on: (a) non-structural parts and other elements, not part of the moment resisting frame, (b) RC member elements of the moment resisting frame. (c) Change in colour of concrete due to exposure to elevated temperature. Observations on the non-structural components were important from the point of view of getting an idea about the level of temperature the surroundings of the RC members were exposed to.

2.3 Field tests

Non-destructive test such as UPV measurements on concrete for a comparative assessment, concrete cover measurement using electromagnetic cover meter, measurement of depth of carbonation front using phenolphthalein indicator solution were conducted. In-situ samples of concrete and reinforcement were also collected for visual inspection and further laboratory investigation. Locations of the building undamaged by fire and samples collected from such locations were treated as control locations/samples in this investigation.

2.4 Laboratory investigations

This involved carrying out laboratory tests on the samples collected from site. Equivalent cube compressive strength of concrete was evaluated by extracting concrete core samples from various locations. Concrete cores of 60 mm diameter were extracted for evaluation of compressive strength, as the maximum size of coarse aggregates as observed visually was found to be about 20 mm. The cores extracted were of sufficient length ranging from 180 mm to 200 mm so as to divide them into two parts. After the core preparation for the compressive strength test, the length of the concrete core was kept in such a manner that L/D (aspect ratio) was between 1 & 2 and cores were tested as per procedure given

in Indian Standard IS: 516. The outer part representing the portion where the effect of exposure to elevated temperature due to fire was likely to be more significant as compared to the inner part. The two parts were tested separately for evaluation of compressive strength. Supplementary laboratory investigations such as Differential Thermal Analysis (DTA), X-Ray Diffraction (XRD) Analysis and Scanning Electron Microscopy (SEM) Imaging were conducted for microstructural characterization & analysis of concrete to support, correlate and validate the results obtained through on-site assessment. Samples of reinforcement steel were also taken from locations affected and unaffected by fire to do a comparative study and assess the deterioration in mechanical properties of steel, if any.

2.5 Classification of damages and recommendations for repair and rehabilitation

Best on the results of the investigations done, conclusions regarding the feasibility of repair were arrived at. The damages to concrete were designated into various damage classes. A detailed location wise survey of the fire damaged portion of building was done to categorize each location into the designated damage classes and accordingly for each class of damage, recommendations on measures to be taken for repair and rehabilitation were given.

3. Post fire condition assessment

3.1 Collection of data related to the building

No documents or drawings other than a basic plan view of the arrangement of rooms on the floors was available. No details regarding the structural design or mix design of concrete were available. Following information was obtained through visual inspection and questioning of on-site personnel: The building under investigation was a RC moment resisting frame system having basement with 6 floors above it (B+G+5). The non-structural internal walls of corridor and internal partition walls between the rooms were made of foam concrete blocks. The ceiling slab consisted of alternating rows of hollow concrete blocks and RC cross beam with the main floor slab being above these. False ceilings were also present in each of the floors and the floors were centrally air conditioned. The year of construction of the building was around late 1950s. The fire took place at the second floor of the building and was first detected in room no.2104. It had caused charring of furniture and services. The fire spread to the floors above through shaft provided inside the rooms for housing the service pipelines. The fire lasted for around 2 hours on the 2nd floor level till the times it was doused. The fire on the 3rd and 4th floor levels was controlled well within time due to which the effect of fire on these floors was negligible. Due to difficulty in accessing the 5th floor, the fire in this floor could not be doused before significant damage was caused by the spread of fire to this floor. The total duration of exposure to fire in the affected floors was around 2 hours.

3.2 Visual survey

3.2.1 Non-structural parts and elements not part of the moment resisting reinforced concrete frame

Charring of the wooden door frames, furniture and deposition of soot was found in almost all the rooms of the fire affected portion of the building. Deformation of glass in doors and windows at locations close to the point where fire was first detected and where duration of exposure to fire was relatively more in comparison to other locations (Fig. 1). Soda lime-silica glass, material with which the window glasses are usually made of, is known to start deforming at a temperature ~ 580 ℃ which indicates that the ambient temperature in these areas had probably breached that mark. Localized softening and partial melting of aluminum in door frames in the vicinity of room where the fire was first detected was noticed (Fig. 2). The melting point of aluminum is known to be about 660.3 oC, which indicates that the external temperature had probably breached this mark at some locations. Rubber hose pipe of fire hydrant at 5th floor level near the staircase entrance (opposite to the end where fire was first detected) had completely melted (Fig. 3). Rubber is known to melt at a temperature of around 180 oC, indicating that temperature in this region had breached this level. The foam concrete blocks of the internal walls in the corridor and the partition walls of the rooms showed excessive cracking and damage (Fig. 4), some of which had become loose. Spalling of the ceiling plaster, the plaster on the beams and columns as well as plaster on the walls was noticed at many locations in 2nd and 5th floors (Fig. 5). The hollow concrete blocks of the ceiling were damaged at some locations and some of these had become dislodged and loose due to disruption of the bond between the blocks and the adjoining concrete of the RC portion (i.e., the cross beams) at the joints between the two (Fig. 6).

Fig. 1 – Deformation of glass in doors and windows

Fig. 2 – Localized softening and partial melting of Aluminum

Fig. 3 – Melting of Rubber hose pipe of fire hydrant

Fig. 4 – Excessive cracking and damage in foam concrete blocks

Fig. 5 – Spalling of ceiling plaster

Fig. 6 – Damaged hollow concrete blocks of the ceiling

3.2.2 Damage to concrete of the reinforced concrete members

Spalling of concrete in the bottom edges of the main longitudinal ceiling beams was observed at some locations close to the room where fire was first spotted (Fig. 7). Delamination of cover concrete in the cross beams (where cover was less) was observed mostly in locations close to the room where fire was first detected (Fig. 8). Spalling of concrete due to corrosion (Fig. 9) was also observed in some of the cross beams of the ceiling near the expansion joints where cover to bottom steel was found to be very less i.e. in the range of 5 to 10 mm as observed visually. Reduction in diameter of the rebar due to corrosion in the range of about 40-50% along the length of the reinforcement bars was observed. Overall, the damage visible on concrete of the columns was found to be less that that observed on the ceiling beams. No noticeable residual deflections at the member level or deformations in the exposed reinforcement bars (other than reduction in diameter at few locations due to corrosion damage) of the RC members were observed anywhere.

Fig.7 – Spalling of concrete in bottom edges of the main longitudinal ceiling beams

Fig.8 – Delamination of cover concrete in the cross beams

Fig.9 – Spalling of concrete due to corrosion

3.2.3 Observations on change in colour of concrete

When concrete gets heated to elevated temperatures, a gradual change in colour of the concrete occurs depending on the temperature range it is exposed to Fib Bulletin 46 (July 2008) [16] gives guidance regarding the probable colour change in concrete depending on the exposure to elevated temperatures (Fig. 10). Change in colour of concrete to pink was found in some of the beams and columns close to the room where fire was first detected (Fig. 11). The depth up to which change in colour of concrete had occurred was also noted on the extracted concrete cores. At locations close to the room where fire was first detected and duration to exposure to fire was more, the maximum depth up to which change in colour of concrete had occurred was found to be about 30-40 mm (Fig. 12). At other locations the colour change was visible only up to about 20 mm depth.

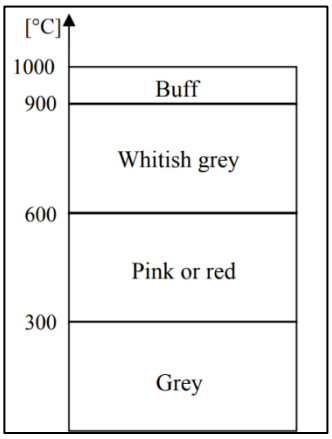

Fig.10 – Colour changes in heated concrete (fib 2008)


Fig.11 – Change in colour of concrete to pink


Fig.12 – Change in colour of concrete at locations close to the room where fire was first detected

3.3 Field Tests

3.3.1 UPV Test

IS 516 (Part 5/Sec 1): 2018 [17] gives guidelines for characterizing the quality of concrete in structures in terms of UPV (Table 1). Out of the nine locations tested by cross probing technique in the fire damaged floors, the quality grading of concrete was found to be doubtful in eight locations and poor in one isolated case (Table 2). It was also seen that the average UPV values for beams obtained by cross probing in the fire damaged floors were somewhat lower than that obtained on the corresponding columns at the same location. The floors where effect of fire was negligible (3rd & 4th floors) were already occupied and operational during the process of field investigation, hence UPV measurements could only be taken by surface probing on these floors. The distribution of UPV values obtained by surface probing is shown in Table 2. As most of the UPV values indicated 'Doubtful' concrete quality grading, UPV measurements were also taken by cross probing technique using 150 kHz transducers on some of the extracted concrete cores taken from the fire damaged floors. The results indicated that the UPV values near the surface region of concrete, where colour change was visible and the effect of exposure to elevated temperatures was likely to be more, typically had lower UPV values as compared to the concrete in the inner regions (Table 3).

Table 1 – Guidelines for characterizing quality of concrete in terms of Ultrasonic Pulse Velocity

S. No	Average Value of Pulse Velocity by Cross Probing (km/s)	Concrete Quality Grading
1	>4.40	Excellent
2	3.75-4.40	Good
3	3.00-3.75	Doubtful*
4	<3.0	Poor

* In case of 'Doubtful' Quality, it may be necessary to carry out further tests

Table 2 – Distribution of UPV values of concrete

Average Value of Pulse Velocity	By cross probing on the Fire damaged floors	By surface probing in Fire Damaged Floors	By surface probing in floors where effect of fire was negligible
< 3 Km/s	1	5	2
3 - 3.75 Km/s	8	1	1
> 3.75 Km/s	-	1	1

Table 3 – UPV values on extracted concrete cores

Depth	UPV values by cross probing on concrete core extracted from ceiling beam of 5th floor	UPV value by cross probing on concrete core extracted from column of 5th floor
20	3.30	3.39
40	3.49	3.41
60	4.20	3.70
80	4.55	3.70
100	4.35	3.97
120	4.51	4.73

3.3.2 Concrete cover study

Measurement of thickness of concrete cover was done using an electromagnetic cover meter. The measured values of concrete cover were compared with specified values given in IS 456: 2000 [18] (Plain and Reinforced Concrete – Code of Practice) which gives the requirement of nominal cover required to meet the specified period of fire resistance. Cover to the outermost bar was found to be less than the requirement of nominal cover required for fire resistance period of 2 hours in 8 out of the 15 locations (Table 4).

3.3.3 Measurement of Depth of carbonation front

Phenolphthalein indicator solution was sprayed onto the concrete cores immediately after extraction to measure the depth of carbonation front. The phenolphthalein indicator solution used for measuring the depth of carbonation front detects reduction in pH (which happens due to consumption of $Ca(OH)_2$. As $Ca(OH)_2$ also dissociates at elevated temperatures, absence of colour on spraying the freshly cut concrete cores with phenolphthalein does not necessarily indicate consumption of $Ca(OH)_2$ due to the normal carbonation reaction. Overall, the depth of 'carbonation front' was found to exceed the concrete cover in 4 out of 17 locations tested (Table 4). In 3rd and 4th floor levels (which were more or less unaffected by fire), the depth of carbonation front was found to vary from 7 to 9 mm.

Table 4 – Average cover and carbonation depth at various locations

Sl. No.	Location	Avg. Cover to outermost bar (mm)	Meeting nominal cover for fire resistance as per Table 16A of IS 456: 2000	Carbonation Depth (mm) Measured on cores of front/side face
1	5th Floor Column	51	Yes	9
2	5th Floor Corridor ceiling beam	Bottom face: 30, Side face: 15	No	15
3	5th Floor Ceiling Beam	Bottom Face: 25，Side face: 29	No	30
4	5th Floor Column	25	No	7
5	5th Floor column	Front Face: 40, Side face: 24	No	15
6	5th floor ceiling beam	Side Face:17	No	30
7	2nd floor column	52	Yes	8
8	2nd Floor Column	35	No	8
9	2nd Floor Ceiling Beam	39	Yes	18
10	2nd Floor Column	44	Yes	9
11	2nd Floor Ceiling beam	34	Yes	20
12	2nd Floor Ceiling beam	46	Yes	12
13	3rd Floor corridor column	68	Yes	8
14	3rd Floor Corridor Column	34	No	7
15	4th Floor corridor column	38	No	9

3.3.4 Concrete core extraction and testing

In order to ascertain the effect of fire damage, if any, on the strength of concrete, cores which were of sufficient length were divided into two halves and the outer half (which represents the portion likely to be affected by exposure to elevated temperatures due to fire) and the inner half (which represents the core concrete of the concerned structural members, on which the effect of exposure of the concrete member to elevated temperatures due to fire is likely to be much less) were tested separately.

All the cores were found to meet the requirement of concrete with minimum compressive strength of 15 MPa. Most of the cores were also found to meet the requirement of concrete with minimum compressive strength of 20 MPa (few cores taken from 2nd floor columns and one core taken from 5th floor ceiling beams did not meet the requirement of 20 MPa compressive strength). It was seen that at most of the locations, the strength of the outer part of the concrete cores extracted from the RC members of the floors affected by fire is not found to be lower than the strength of the inner part of the core. Higher strength of outer part at some locations may be on account of formation of calcium carbonate due to carbonation of concrete and in some measure due to densification at microscopic level as a result melting of certain components which then subsequently fill the pores. Strength of the cores extracted from the vicinity of the room where fire was first detected is found to be relatively lower compared to other locations. However, it cannot be conclusively said that this reduced strength is due the effect of fire as no significant reduction in strength of outer part of core as compared to the inner part is seen.

3.4 Laboratory investigations

3.4.1 Differential Thermal Analysis (DTA)

The most widely used thermal method of analysis is DTA. In DTA, the temperature of a sample is compared with that of an inert reference material during a programmed change of temperature. The temperature should be the same until thermal event occurs, such as melting, decomposition or change in the crystal structure.

Fig.13 – Extraction of concrete core from column of fire damaged floor

Fig.14 – Demarcation of concrete core into two parts (A & B) for separate testing of outer and inner part

If an endothermic event takes place within the sample, the temperature of the sample will lag behind that of the reference and a minimum will be observed on the curve. On the contrary, if an exothermal event takes place, then the temperature of the sample will exceed that of the reference and a maximum will be observed on the curve. The area under the endotherm or exotherm is related to the enthalpy of the thermal event, ΔH. Peaks can be observed in the DTA curve whenever an exothermic or endothermic event takes place. In order to carry out DTA, concrete powder samples were obtained at various ranges of depths from the outer concrete surface. $Ca(OH)_2$ is known to dissociate at around 450^0C-550^0C whereas carbonates decompose at temperature range of about 700^0C-900^0C. In concrete already exposed to such elevated temperatures, the endothermic peaks corresponding to disassociation of these components will be absent on the DTA curve. Peaks corresponding to decomposition of carbonates were observed in all of the DTA curves. This indicates that the exposure temperature of concrete did not breach the 700^0C mark in any portion of the RC members. For 3rd floor, where effect of fire was negligible, peak due to dissociation of $Ca(OH)_2$ was absent in the DTA curve at 0-5 mm depth whereas it was present in the DTA curves at greater depths. This indicates that at 0-5 mm depth, the peak was absent because of carbonation of concrete (measured depth of carbonation front was found to be about 7 mm) and not due to exposure to elevated temperatures due to fire (Fig. 15 & 16). As carbonation had not progressed beyond this depth, the peaks corresponding to dissociation of $Ca(OH)_2$ were present in the DTA curves at greater depths. For 2nd floor column, peak corresponding to dissociation of $Ca(OH)_2$ were absent in the DTA

curves up to 19 mm depth whereas the peaks were present in the DTA curves at greater depths (Fig. 17 & 18). This indicates that the absence of $Ca(OH)_2$ dissociation peak up to 19 mm depth is due to exposure to elevated temperature due to fire whereas at greater depths the peaks are present as the exposure temperature was at a much lower level. Same was also seen from the depth of the colour change to pink as observed on the extracted concrete cores. For some of the ceiling beams, peak corresponding to dissociation of $Ca(OH)_2$ were absent up to 30-40 mm depth whereas they were present at greater depths. Depth of colour change to pink was also observed up to 30-40 mm depth on the extracted concrete cores. This again indicates that the peaks were absent due to exposure to elevated temperatures due to fire whereas at greater depths the peaks were present as the exposure temperature was at a much lower level.

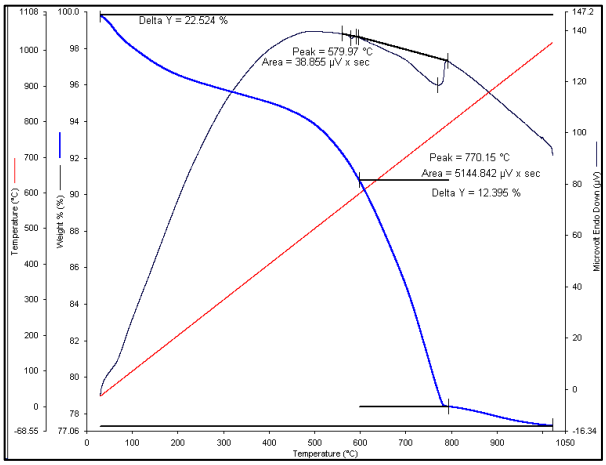

Fig. 15 – DTA curve for 3rd floor corridor column (unaffected by fire) at 0-5 mm depth wherein peak due to decomposition of $Ca(OH)_2$ is absent – due to carbonation

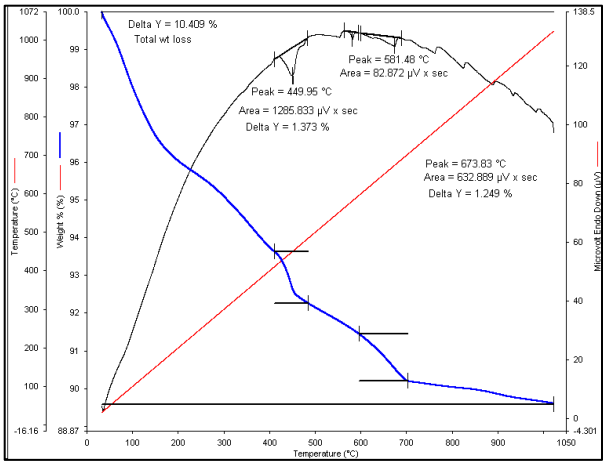

Fig.16 – DTA curve for 3rd floor corridor column (unaffected by fire) at 7-12 mm depth wherein peak due to decomposition of $Ca(OH)_2$ is present

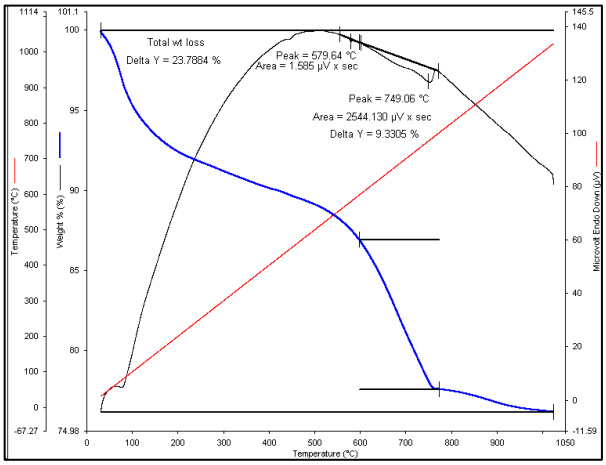

Fig.17 – DTA curve for 2nd floor column outside room where fire was first spotted at 14-19 mm depth

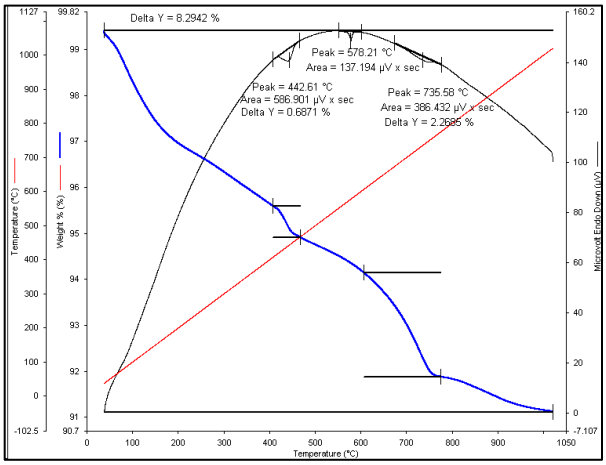

Fig.18 – DTA curve for 2nd floor column outside room where fire was first spotted at 21-26 mm depth

3.4.2 Scanning Electron Microscopy (SEM) imaging

Scanning electron microscopy is a technique for achieving high resolution images of surfaces. It involves scanning a fine beam of electrons over a specimen and detecting the signals which are emitted. The SEM uses a focused beam of high-energy electrons to generate a variety of signals at the surface of solid specimens. The signals that derive from electron-sample interactions reveal information about the sample including external morphology (texture), chemical composition, and crystalline structure and orientation of materials making up the sample. In most applications, data are collected over a selected area of the surface of the sample, and a 2-dimensional image is generated that displays spatial variations in these properties. Areas ranging from approximately 1 cm to 5 microns in width can be imaged in

a scanning mode using conventional SEM techniques (magnification ranging from 20X to approximately 30,000 X, spatial resolution of 50 to 100 nm). SEM imaging enables one to view the microstructure of concrete samples at different depths at very high magnifications levels and also assess the presence or absence of portlandite crystals which appear in the form of hexagonal plate like structures in the SEM micrographs. The effect of exposure to high temperatures on the microstructure can be analyzed by observing the SEM micrographs at different depth levels. Exposure to high temperature is likely to cause the microstructure to become relatively loose and result in the appearance of higher pore sizes and microcracks. In samples taken from third floor column, the SEM images indicate that in depth range of 0-5 mm (Fig. 19), negligible portlandite is seen in the SEM micrographs, whereas presence of portlandite in the form hexagonal plate like morphology is clearly seen in 7-12 mm depth (Fig. 20) which correlates with the DTA results. In samples taken from 2nd floor column, no portlandite is seen up to 14-19 mm depth (Fig. 21) and the microstructure is also found to be relatively less dense. In 21-26 mm depth, portlandite is found (Fig. 22). No major sized voids are found in this depth and the microstructure is found to be relatively denser. In SEM micrographs of samples taken from one of the fifth ceiling beams, the microstructure is found to be less densified up to a depth of 30-40 mm from the surface with presence of micro cracks and clustered micro pores with irregular shape. Hexagonal morphology is also found to be absent up to this depth in the SEM micrographs. At 40-50 mm depth from the surface, the microstructure is found to be relatively denser as compared to the other samples and number of micro cracks at this depth is also found to be fewer in number as compared to the other samples. The depth up to which concrete was found to be affected as indicated by the DTA results was generally in agreement with the appearance of microstructure at various depths as indicated by the SEM micrographs.

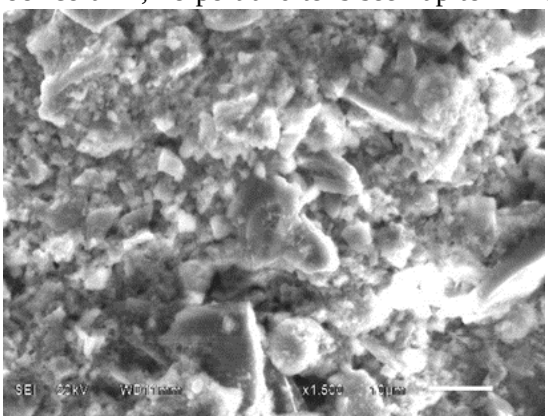

Fig.19 – SEM images of samples from 3rd floor column, from in depth range of 0-5 mm. Hexagonal morphology is absent. Microstructure found to be relatively less densified and porous

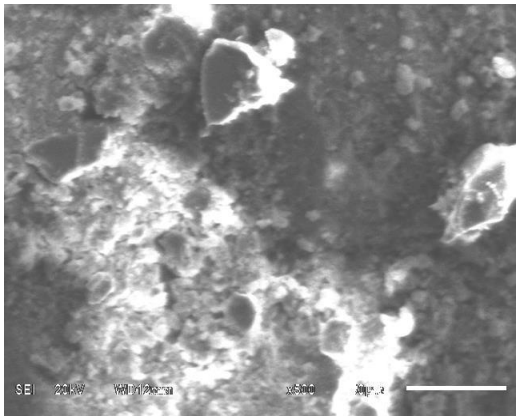

Fig.20 – SEM images of samples from 3rd floor column, from in depth range of 7-12 mm Hexagonal morphology is absent. Microstructure found to be relatively less densified and porous

3.4.3 X-Ray Diffraction (XRD) analysis

X-ray powder diffraction (XRD) is a rapid analytical technique primarily used for phase identification of a crystalline material and can provide information on unit cell dimensions. The analyzed material is finely ground, homogenized, and average bulk composition is determined. Crystalline substances act as three-dimensional diffraction gratings for X-ray wavelengths similar to the spacing of planes in a crystal lattice. XRD is now a common technique for the study of crystal structures and atomic spacing. XRD is based on constructive interference of monochromatic X-rays and a crystalline sample. These X-rays are generated by a cathode ray tube, filtered to produce monochromatic radiation, collimated to concentrate, and directed toward the sample. The interaction of the incident rays with the sample produces constructive interference (and a diffracted ray) when conditions satisfy Bragg's Law ($n\lambda=2d \sin \theta$). This law relates the wavelength of electromagnetic radiation to the diffraction angle and the lattice spacing in a crystalline sample. These diffracted X-rays are then detected, processed and counted. By scanning the sample through a range of 2θ angles, all possible diffraction directions of the lattice should be attained due to the random orientation of the powdered material. Conversion of the diffraction peaks to d-spacings allows identification of the mineral because each mineral has a set of unique d-spacings. Typically, this is achieved by comparison of d-spacings with standard reference patterns.

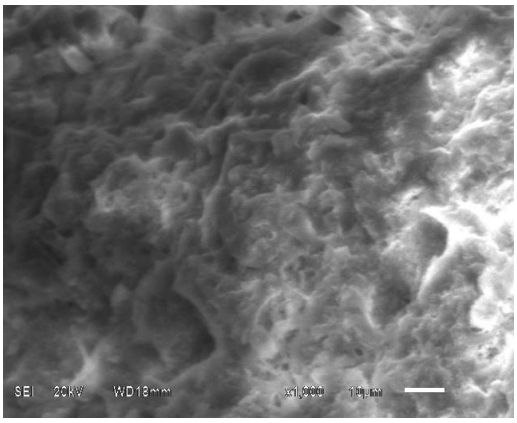

Fig.21 – SEM images of samples from 2nd floor column, from depth range of 14-19 mm depth. Presence of hexagonal morphology indicating the probable presence of portlandite

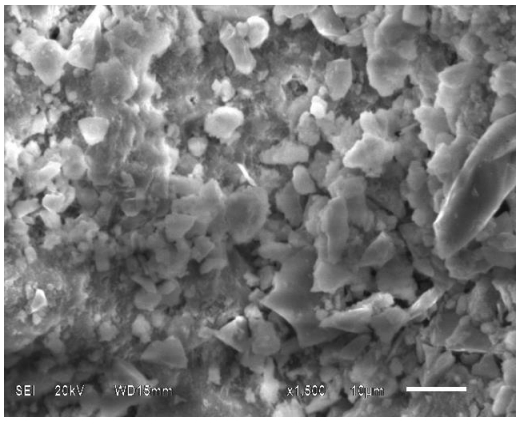

Fig.22 – SEM images of samples from 2nd floor column, from depth range of 21-26 mm depth. Hexagonal morphology is absent. Microstructure found to be less densified with presence of micro pores and micro cracks

In the present study, slices at varying depths from the extracted concrete cores were obtained by sawing. The mortar/paste portion was then ground to powder form and the evaluation of powdered samples was carried out using XRD technique. In all the samples across various depths, quartz is found to be in predominant abundance. This is due to presence of fine aggregate of the mortar portion which is difficult to separate. In samples of 0-5 mm depth (Fig. 23), portlandite is found to be absent in samples taken from C48 (3rd Floor column), C24 (2nd floor column) and C4 (5th floor column). In samples taken from 7-12 mm depth (Fig. 24), peaks in the XRD pattern corresponding to portlandite in minor abundance are seen in sample of C48 where is in samples of C24 and C4, they are absent. In samples taken from 14-19 mm depth (Fig. 25), calcite ($CaCO_3$) is found to be in relatively major abundance in sample taken from C24 whereas peak corresponding to portlandite is absent. On the other hand, peaks indicating portlandite in minor abundance are seen XRD pattern of C48 & C4 in this depth. In 21-26 mm depth (Fig. 26), peaks indicating portlandite in minor abundance are seen in samples taken from C48, C4 as well as C24. It is seen that the results of XRD analysis are in accordance with the results of DTA and SEM.

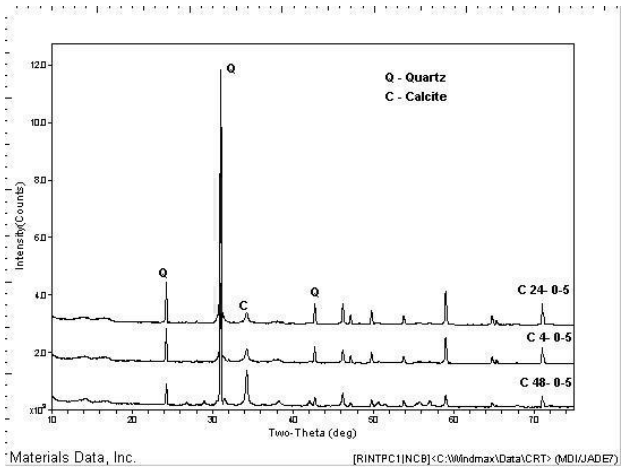

Fig. 23 – XRD images of samples from C48 (3rd floor column), C24 (2nd floor column) and C4 (5th floor column) from in depth range of 0-5 mm

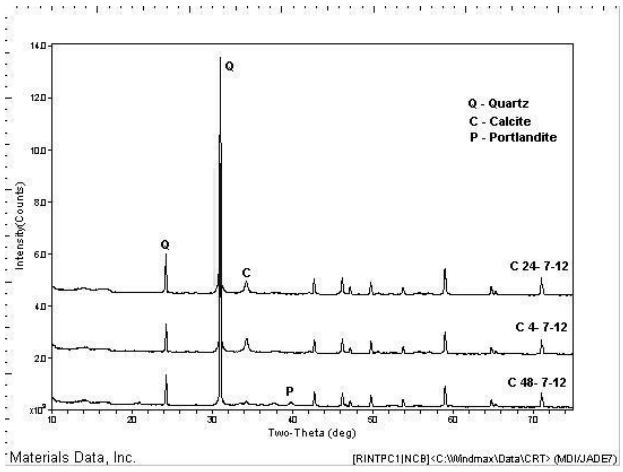

Fig.24 – XRD images of samples from C48 (3rd floor column), C24 (2nd floor column) and C4 (5th floor column) from in depth range of 7-12 mm

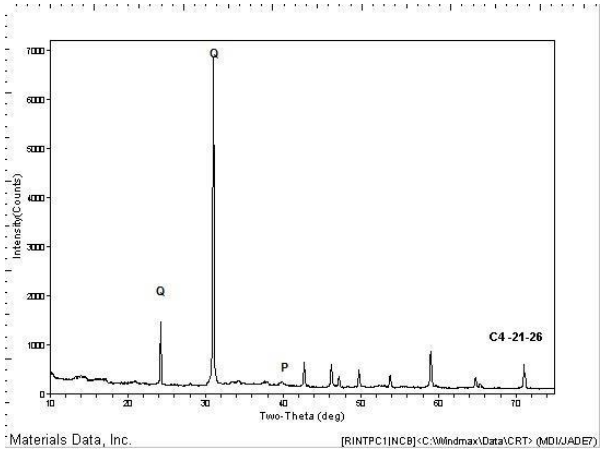

Fig 25 – XRD images of samples from C48 (3rd floor column), C24 (2nd floor column) and C4 (5th floor column) from depth range of 14-19 mm depth

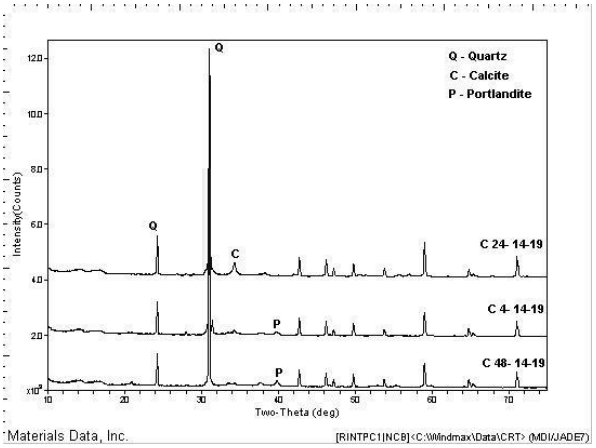

Fig 26 – XRD images of samples from C48 (3rd Floor column) from depth range of 21-26 mm depth

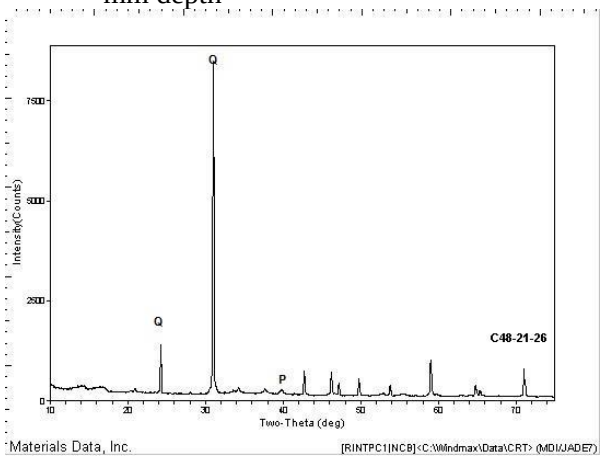

Fig 27 – XRD images of samples from C4 (5th floor column) from depth range of 21-26 mm depth

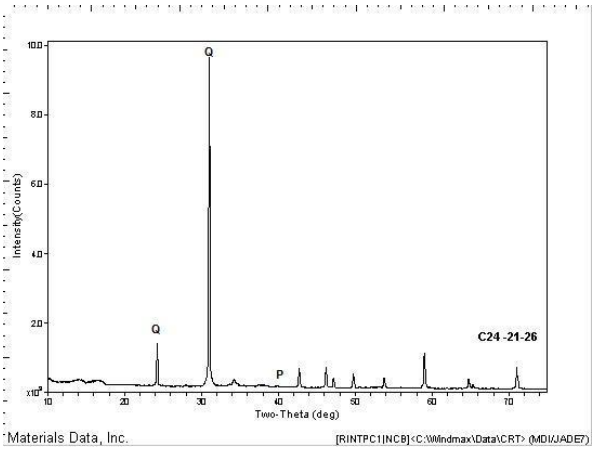

Fig 28 – XRD images of samples from C24 (2nd floor column) from depth range of 21-26 mm depth

3.4.4 Optical Microscopy (OM) analysis

An optical microscope creates a magnified image of an object specimen with an objective lens and magnifies the image further more with an eyepiece to allow the user to observe it by the naked eye. An optical microscope consists of two major basic functions (a) Creating a Magnified Image of a Specimen (b) Illuminating a specimen. Optical Microscope images/micrographs allow the study of mircrostructure of samples prepared at low magnification.

The OM micrographs of the undamaged concrete sample due to fire taken from 3rd floor column (Fig. 29) have indicated the presence of closed voids with deposited hydrated products with relatively smooth margins and compactness of mortar and aggregate. The OM micrographs of the samples taken from fire damaged floors on the other hand have indicated presence of greater number microcracks (Fig. 30) and formation of micro cracks in cement mortar and at the interface of aggregate and cement mortar (Fig. 31 and Fig. 32) which may be due to effect of heating. The microscopic investigation of the fire damaged cores indicated that the distribution pattern of the grains and pores spaces changed drastically. Even the morphology of the grains of the fine aggregate component was also changed. Large variation was noticed in air void distribution pattern from the front to inside portion. Bottom portion was directly exposed to fire, which had caused sealed walled air voids bigger in size. Size of pores after fire might have increased but have very stable and firm walls, which had presently helped to achieve more strength to the concrete. As the tracking of microscopic analysis gone inside the core, size of air voids reduced drastically. However, partial melting of fine aggregate component was noticed in these areas. The same was seen from SEM Study results also when the samples were compared from fire damaged portion and sample from the concrete portion unaffected by the fire.

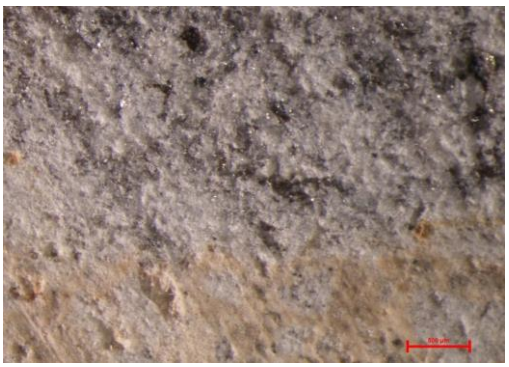

Fig. 27 – Third floor column with Compactness of mortar with aggregate (30X)

Fig. 28 – Development of micro cracks at the base of void from fire damaged concrete (15X)

Fig. 29 – Formation of micro cracks in cement mortar and at the interface of aggregate and cement mortar (45X)

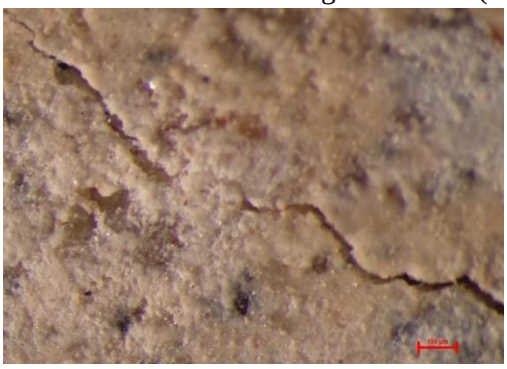

Fig. 30 – Formation of micro cracks in cement mortar and at the interface of aggregate and cement mortar (90X)

3.4.5 Effect of fire on mechanical properties of reinforcement steel

Sample of reinforcement steel was taken from a landing slab of fire affected 5th floor staircase and from landing slab of an adjacent block which was unaffected by fire (which is treated as reference sample) to get an idea of the effect of exposure to elevated temperature on the mechanical properties of reinforcement steel (Table 5). It may be noted that all reinforcement in the structure is of mild steel. Samples from both locations were tested for different physical properties of reinforcement made of mild steel as per BIS specifications. Is comparison to the reference sample (which is unaffected by fire), there has been a reduction in the mechanical properties of the reinforcement steel sample taken from the fire affected area. Cover to reinforcement in beams at some places is found to be less than 30-40 mm (mostly in the case of ceiling beams), and effect of elevated temperature as ascertained through results of DTA and SEM micrographs was found to be up to 40 mm in some cases for the ceiling beams. This points towards the need for strengthening, especially for the flexural members.

Table 5 – Mechanical properties of reinforcement steel

Location of Reinforcement sample	Yield stress	Tensile strength	Young's Modulus
From landing slab of fire damaged floor	285.17 MPa	460.33 MPa	169.81 GPa
From landing slab of adjacent block unaffected by fire	321.16 MPa	549.25 MPa	226.35 GPa

3.4.6 Repair and rehabilitation methodology adopted

Based on the visual inspections indicating the condition of surface and structural elements such as spalling, exposure and condition of reinforcement, cracks, honeycombing etc. along with NDT evaluations / laboratory test results, the structural members were repaired using methodology given below:

- Firstly, removal of plaster/paint on the surface of the members and chipping off and removal of all loose/delaminated concrete. Detection and removal of loose concrete was done by striking the

concrete surfaces with a 2lb hammer. Sand blasting and water jet was also be used for removal of loose material where required.

- If after chipping work, any honeycombed portions or cracks are visible on the concrete surface, injection grouting using low viscosity, high strength polymeric resin/monomer based grout (which becomes rigid on setting) was carried out after removal/chipping of loose/delaminated concrete.
- Prior to carrying out grouting for cracks along their length, cutting of V-notches along the length of the cracks was done. The space around the grouting notch and the injection nozzle was sealed using epoxy mortar/epoxy putty and the same was allowed to cure and harden prior to starting the grouting process. A curing time of around 24 hours is usually sufficient.
- The injection nozzles for grouting was arranged in a staggered fashion at spacing of about 300 mm c/c. The grouting proceeded from the lower to the upper nozzles. The injection process proceeded from the lowest nozzle and should be injected from the lower nozzle at required pressure (usually between 3.5 to 7 kg/cm^2) using a grout pump and the injection process should continue till grout is seen oozing out from the upper nozzle or till the grout pump receives no further grout and the grouting pressure starts increasing suddenly. After that, the grouting pressure was maintained for about 30 seconds – 1 minute, and subsequently the nozzle was cut off and the grout injection point sealed using suitable repair mortar (epoxy mortar or epoxy putty will suffice).
- After execution of chipping and grouting wherever required, the replacement of the lost section of concrete was done using polymer modified mortar (PMM) system or prepacked micro concrete. Before replacement of lost section using PMM/prepacked micro concrete, a bond coat should be applied on the old concrete substrate to ensure proper adhesion of the repair material. For bonding the freshly prepared mortar/prepacked micro concrete to the old concrete substrate, epoxy bond coat should be used. Prior to building up the lost section using PMM, the following steps need to be completed:
  - Where rebars are found to be corroded, cleaning of reinforcement of rust and loose scale using alkaline rust remover was done. This was followed by application of anticorrosive coating on reinforcement steel.
  - As pH value has reduced in the surface region at some locations as a result of exposure to elevated temperature due to fire, and total acid soluble chloride content was also more than 0.6 kg/m^3 at most locations, application of surface applied concrete penetrating corrosion inhibitor which works by bipolar mechanism to minimize further de-passivation of reinforcement steel was applied.
  - Fixing of additional reinforcement wherever reduction in diameter of rebar due to corrosion is found to be more than 10% was done as part of repair system prior to building up the profile of the members by polymer modified mortar/prepacked micro concrete. Visible reduction in cross section of the reinforcement steel, particularly the stirrups, was observed in some of the cross beams of ceiling at 5th floor level and therefore, additional steel will was recommended at these locations.
  - The additional reinforcement was secured in place to the existing reinforcement with steel shear anchors. It was recommended to use steel shear anchors as welding may have an effect on the thermo-mechanical properties of steel.
- Strengthening of severe damaged RCC ceiling beams (both longitudinal and cross) was done with non-metallic composite fiber wrapping system comprising of uni-directional E-glass fiber (900 Grams per Square Meter (GSM)) wrap and compatible epoxy saturant, by wet lay-up system by applying compatible primer on prepared substrate. FRP wrapping of beams was done after carrying out all normal repair works as described above. Before execution of fiber wrapping, the edges of the rectangular beams should be rounded off (to a minimum of 25 mm radius) by chamfering.

4. Conclusions

Based on above mentioned study, following conclusions were drawn**:**

a) Based on visual inspection and results of field and laboratory investigations, the maximum depth to which concrete was affected by fire was found to be about 20 mm for columns and about 30-40 mm for ceiling beams. Equivalent cube compressive strength of concrete was found to meet the requirement of concrete with minimum compressive strength of 15 MPa at all locations and 20 MPa compressive strength at most of locations. The maximum temperature to which concrete in the structural members was exposed was generally less than 700^0C as de-carbonation peak was observed in all the DTA curves. Some deterioration in the mechanical properties of reinforcement steel sample taken from fire affected area as compared to that of an area unaffected by fire was observed. Corrosion damage

to reinforcement steel was observed at some locations. Based on the findings, the structural members affected by fire were found to be fit for repair.

b) Based on the visual inspections, field and laboratory test results, the structural members were repaired by chipping off loose, delaminated and fire damaged portions and subsequent replacement with PMM system or micro concrete depending extent of damage. The supplemental reinforcement was provided where reduction in diameter of reinforcement was found to be more than 10% and treatment of the existing corrosion damaged reinforcement was done to minimize chances of further corrosion.The strengthening of the beams and members where UPV values by cross probing were found to be less than 3.00 km/s by FRP wrapping was recommended.

References

1. Chiang, Chih-Hung and Tsai, Cho-Liang, "Time-Temperature Analysis of Bond Strength of a Rebar after Fire Exposure, "Cement and Concrete Research," V. 33, No. 10, Oct. 2003 pp 1651-1654
2. Edwards, William T. and Gamble, William L., "Strength of Grade 60 Reinforcing Bars After Exposure to Fire Temperatures," Concrete International, V.8, No. 10, Oct. 1986, pp. 17-19
3. Benedetti A, "Ultrasonic Pulse Propagation into Fire-Damaged Concrete" ACI Structural Journal, (1998) V.05, No.5, pp. 259 - 270.
4. Chung H W & Low K S, "Assessing fire damage of concrete by the Ultrasonic Pulse Technique", American Society of Testing & Materials (1985), pp. 84- 88
5. Cioni P, Croce P & Salvatore W, "Assessing fire damage to R.C. elements". Fire safety Journal (2001), p. 181 – 199
6. Lin W M, Lin T D & Couche L J P "Microstructure of Fire Damaged Concrete" ACI Materials Journal (1996), V.03, No.3, pp.199-205
7. Short N. R., Purkiss J. A., & Guise, S.E., "Assessment of fire damaged concrete", Construction and Building Materials (2001), Vol.15, pp. 9-15.
8. Georgali B & Tsakiridis P E, "Microstructure of fire damaged concrete - A case study", Cement and Concrete composites (2005), Vol.27, pp.255-259
9. Gosain N. K., Drexler F. Ray & Choudhuri Dilip, "Evaluation and Repair of Fire Damaged Buildings", Structure Magazine, (2008), pp.18-22
10. Osman M. H., Sarbini N. N., Ibrahim I. S., Ma C. K., Ismail M. & Mohd M. F. "A case study on the structural assessment of fire damaged building" 2017 IOP Conf. Ser.: Mater. Sci. Eng. 271,012100
11. Ha, T., Ko, J., Lee, S., Kim, S., Jung, J. and Kim, D.J. (2016), "A case study on the rehabilitation of a fire-damaged structure", Appl. Sci., 6(5), 126
12. Emmanuel V.R.A & Luc R. T., "Assessment techniques for the evaluation of concrete structures after fire" Journal of Structural Fire Engineering 4(2), pp. 123-129
13. Brancaccio A, Serafini R & Casadei R, "In-situ structural assessment and FRP strengthening of a fire damaged RC structure: A case study". Proceedings of the 6th International Conference on FRP Composites in Civil Engineering, Rome, Italy, June (2012) pp.13 - 15
14. Liu M, Fan X H, Zuo Y Z & Song G F, "Strengthening and retrofitting of the industries building after fires" Advanced Material Research (2013), p. 671 - 674
15. Thi C N, Pansuk W & Torres L "Flexural behavior of fire-damaged Reinforced Concrete slabs repaired with near-surface mounted CFRP rods". Journal of Advanced Concrete Technology (2015), 13, p. 15 - 29
16. Fib Bulletin 46, State-of-art report on "Fire design of concrete structures – structural behavior and assessment", July (2008)
17. IS 516 (Part 5/Sec 1): 2018, "Hardened Concrete - Methods of Test, Part 5: Non-Destructive Testing of Concrete, Section 1: Ultrasonic Pulse Velocity Testing". Bureau of Indian Standards, New Delhi, India (2018)
18. IS 456: 2000, "Plain and Reinforced Concrete: Code of Practice". Bureau of Indian Standards, New Delhi, India (2000)